Auxetic materials for MEMS: modeling, optimization and additive manufacturing

Valentina Zega[1], Matteo Bruggi[1], Marinella Levi[2], Alberto Corigliano[1]
[1] *Department of Civil and Environmental Engineering, Politecnico di Milano, Milan, Italy*
E-mail: valentina.zega@polimi.it, matteo.bruggi@polimi.it, alberto.corigliano@polimi.it

[2] *Department of Chemistry, Material and Chemical Engineering "Giulio Natta", Politecnico di Milano, Milan, Italy*
E-mail: marinella.levi@polimi.it

Keywords: auxetic-materials, MEMS, 3D-printing

Auxetic materials are of interest because of enhanced material properties related to negative Poisson's ratio, such as increased shear modulus, indentation resistance, fracture toughness, energy absorption, porosity/permeability variation with strain and synclastic curvature.

In addition, the Poissons ratio does not depend on scale: deformation can take place at the nano- (molecular), [1], micro-[2], or even at the macro-level, [3]; the only requirement is the right combination of the geometry and the deformation mechanism.

The most popular feature of auxetic structures is that it can expand in the direction perpendicular to an externally exerted tension. This property makes auxetic structures strongly appealing for MEMS applications (i.e. motion conversion and resonators) [4].

Here we present a full study of a re-entrant honeycomb structure which can be used in MEMS devices as motion conversion spring. The design of the proposed structure is obtained from a Matlab© optimization procedure targeted to reach a Poisson's ratio equal to -1. An additional nonlinear numerical simulation (see [5]) is done to verify the behavior of the structure under large deformations regime, which is the one required by the MEMS applications and then, a 3D-printed model (see [6]) of the optimized structure is obtained.

Finally, a topology optimization is performed to obtain an auxetic structure that, in principle, can amplify the motion in the direction othogonal to the driving one. With this procedure there is no need to create an input structure from which the optimization procedure can start. Also for one of these optimized auxetic structures, an additional nonlinear numerical simulation is done.

1 Introduction

In Micro Electro Mechanical Systems (MEMS) usually there is the need to have the simultaneous motion of the masses in more than one direction for example in tri-axis gyroscopes (i.e. [7] and [8]). Three axis gyroscopes need at lest two orthogonal driving directions and a linear behavior in both axes; in addition, very often, it is not possible to actuate the two directions and, as a conseguence, a complex spring configuration for the conversion of the motion is needed.

So the key issue is to have actuation in only one direction and resultant driven motion in two directions (see [9] for example).

Here we present some possible solutions to this problem through auxetic structures. The most popular feature of auxetic structures is, in fact, that it can expand in the direction perpendicular to an externally exerted tension. In addition, they enhance material properties related to negative Poisson's ratio, such as increase shear modulus, indentation resistance, fracture toughness, energy

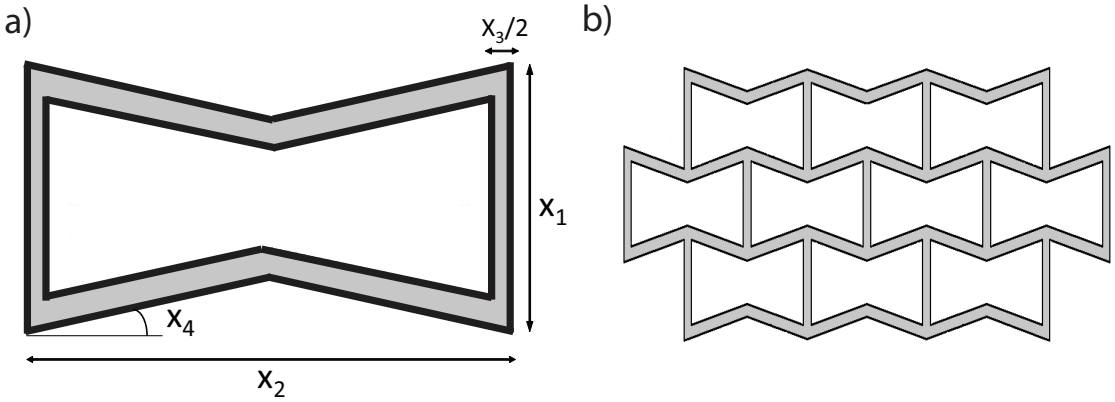

Figure 1: Re-entrant honeycomb structure to be optimized. a) Unit cell of the auxetic structure: the geometrical variables used during the optimization procedure are shown; b) full re-entrant honeycomb structure composed by ten unit cells.

absorption, porosity/permeability variation with strain and synclastic curvature. For these reasons auxetic structures seem very promising for MEMS design.

These structure despite being theoretically applicable for in-plane motion conversion, cannot be used for out of plane motion conversion: they require particular out of plane section which, up to now, are incompatible with the standard MEMS fabrication processes (i.e. [10]).

To solve that problem, we propose a new fabrication process: the 3D-printing process. This kind of fabrication is fastly devoloping and in a short time it could reach the very small dimensions related to the MEMS world. In this paper we show some 3D-printed prototypes at the mesoscale, but additional work will be done in the direction of decreasing the dimensions.

2 Optimization of a re-entrant honeycomb structure

The most popular auxetic structure (see [4] and [11]) is the re-entrant honeycomb structure (see Figure 1b) because of its very simple shape and its good auxetic properties.

In this section we start from the re-entrant honeycomb structure and proceed through an optimization procedure.

We use the interior point algorithm of the optimization toolbox of Matlab© combined with a FEM (Finite Element Method) code to reach the best auxetic structure which has Poisson's ratio equal to -1.

We apply a prescribed displacement along the x-direction, we compute the displacement in the y-direction through the FEM beam code and we minimize the difference between the two displacements.

The objective function of the optimization code is, in fact, the difference between the displacement imposed in the x-direction and the displacement we obtain in the orthogonal y-direction because of the auxetic behavior of the strucure: minimizing the objective function, we are imposing the Poisson ratio equal to -1 as whished.

The optimization variables are the geometrical parameters of the unit cell shown in Figure 1a.

They are:

- x_1: height of the unit cell of the structure;
- x_2: lenght of the unit cell of the structure;
- x_3: width of the unit cell of the structure;
- x_4: inclination of the inclined parts of the unit cell of the structure.

To make the structure feasible some geometrical constraints must be imposed (i.e. the no-compenetrability of the single components of the structure) together with some lower and upper bounds for the values of the different variables.

In table 1 we show the results of the optimization code for constraint of the form:

$$\frac{x_2}{2}\tan(x_4) - \frac{x_1}{2} \leq 0 \tag{1}$$

$$2x_3 - x_1 + 30 \leq 0 \tag{2}$$

$$2x_3 - x_2 + 60 \leq 0 \tag{3}$$

and upper and lower bounds equal to:

$$x_{up} = [1500 \quad 1500 \quad 300 \quad 80^\circ]; \qquad x_{low} = [30 \quad 30 \quad 30 \quad 10^\circ]; \tag{4}$$

Note that the upper bounds shown in (4) are very high with respect to the classical dimensions of MEMS world. Here the only purpose is to show if that procedure can work also for MEMS applications. After that stage, a MEMS compatible design can be done.

Table 1: Optimized geometrical parameters of the unit cell of a re-entrant honeycomb structure studied.

x_1	x_2	x_3	x_4
630 μm	660 μm	30 μm	0.174 rad

2.1 Non-linear analysis of the optimized structure

As anticipated in the Introduction, the linear behavior of MEMS structure is desirable also for large displacements of the proof mass (i.e. driven motion of gyroscopes), as a conseguence, a further numerical analysis is required to validate the results of the optimization procedure carried out under the hypothesis of small displacements.

A non-linear FEM model is done in ANSYS© and in Figure 2a we show the good results of the optimization procedure also in the non-linear regime: the displacement in the direction orthogonal to the one where we impose the displacements are equal to the imposed one and this means that the Poisson ratio of our structure is equal to -1.

In Figure 2b we report the force-displacement relation for different values of the imposed x-axis displacement. Here we can see that, for displacements of the order of some micrometers, the relation between force and displacements is linear. This means that our optimized structure can work as linear motion converter and can consequently be used in MEMS devices like gyroscopes.

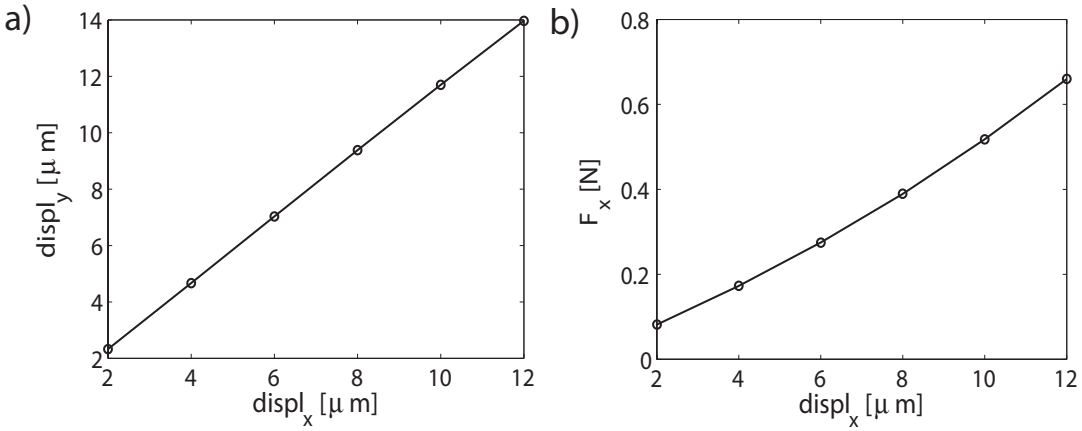

Figure 2: Non-linear numerical analysis of the optimized auxetic structure (numerical values are computed using the polysilicon as material). a) Imposed x-axis displacements versus computed y-axis displacement: the relation is linear and that proves the results of the optimization procedure; b) imposed x-axis displacements versus computed x-axis reaction forces: for displacements of the order of some micrometers the relation is linear (fitting curve: $y = -9 \cdot 10^{-7}x^4 + 4 \cdot 10^{-5}x^3 + 0.001x^2 + 0.0386x$)

2.2 3D-printed prototypes of the optimized structure

After the full study of the optimized auxetic structure, a first prototype is produced through the 3D-printing technique. The 3D-printing is a rather new technology for the MEMS world and it could release a lot of the actual fabrication constraints. Despite the fact that up to now we are not able to produce very small structures, we are quite confident in the possibility to reach that target in the near future.

In Figure 3 we show two 3D-printed prototypes: they live in the mesoscale because of the before mentioned reasons but the behavior is exactly the same as the one of the optimized structure because the Poisson's ratio does not depend on the overall dimensions of the structure.

The two prototypes are made of DL 260 Moulding Resin whose Young's modulus is in the range of 2-3 GPa and they are scaled of a factor of 25 and 12.5 with respect to the values reported in Table 1. Measurements on the prototypes are still in progress.

3 Topology optimization of an auxetic structure

The main problem of the previous optimization procedure is the need to have an initial structure to be optimized. We want now to move towards the topology optimization that can maximize the ratio between the y-axis displacements obtained as a conseguence of the imposed displacements in the x-direction without starting from an initial configuration. Maximizing that ratio we are minimizing the Poisson's ratio which now can become much smaller than -1. We are consequently looking for a conversion and amplification of motion.

Classical formulations of topology optimization distribute a prescribed amount of isotropic material in order to minimize the so-called structural compliance, which is the work of the external forces

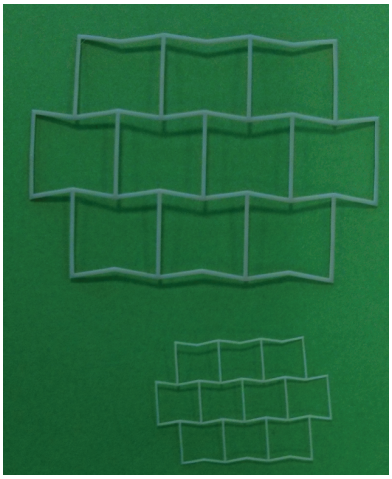

Figure 3: Two 3D-printed prototypes of the optimized re-entrant honeycomb structure shown in Figure 1b. The dimensions of the two prototypes are the ones reported in Table 1 multyplied by a factor of 25 and 12.5 respectively.

at equilibrium [12]. Minimizing the structural compliance is in turns equivalent to minimizing the overall elastic strain energy, that means looking for the stiffest way to bear the load.

Alternatively, formulations of topology optimization can be adopted to perform the synthesis of compliant mechanisms, i.e. finding the distribution of material that maximizes the output displacement u_{out} applied to a workpiece for an input displacement enforced elsewhere through an actuator [13].

Let us consider a domain made of a linear elastic body that is discretized through a finite element grid made of N elements. Assuming, for simplicity, that the input actuator is a linear strain based actuator, it can be modeled resorting to a spring (called input spring in the follow) with stiffness k_{in}. The output workpiece is modeled thorough a spring (called output spring in the follow) with stiffness k_{out}, herein equal to k_{in}. Assuming low stiffness of the input/output springs with respect to the domain to be optimized, conventional mechanisms arise that are made of members connected through hinges. Increasing such a parameter, stiff structures are found that maximize the output displacement u_{out} with no articulation. The latter setup is employed in the following setting to maximize u_{out}:

$$\begin{cases} \max\limits_{x_{min} \le x_e \le 1} & u_{out} \\ \\ \text{s.t.} & \sum\limits_{e}^{N} x_e^p \mathbf{K}_{0e}\, \mathbf{U}_e + k_{in} u_{in} + k_{out} u_{out} \;=\; \mathbf{F}, \\ & \mathcal{W} \,/\, \mathcal{W}_0 \;\le\; V_f, \end{cases} \tag{5}$$

In the above relation, the objective function is the output displacement u_{out}, Eqn. $(5)_2$ enforces the discrete equilibrium under the assumption of linear modeling and Eqn. $(5)_3$ enforces the volume constraint.

The element stiffness matrix computed for the virgin material $\mathbf{K}_{0e}$ is scaled through the term x_e^p (with $p = 3$) that implements the so called Solid Isotropic Material with Penalization (SIMP),

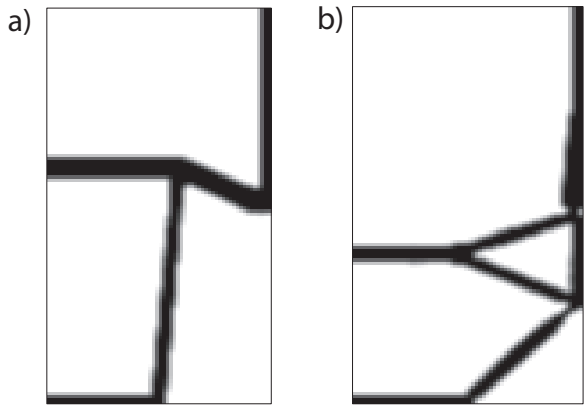

Figure 4: Two possible optimized auxetic structures obtained through topology optimization: they differ from each other for the boundary conditions. a) Optimized auxetic structure obtained with only one input spring and only one output spring, b) Optimized auxetic structure obtained with three input spings and three output springs.

interpolating the stiffness of the continuum depending on the density unknowns x_e [14]. A lower bound $x_{min} > 0$ is enforced on each density unknown x_e to avoid singularity of Eqn. $(5)_2$.

The weight $\mathcal{W}$ is computed multiplying x_e for the volume V_e over the N elements in the discretization, whereas $\mathcal{W}_0$ stands for the volume of the whole design region. The available material is prescribed as a percentage through the volume fraction V_f.

The formulation in Eqn. (5) is solved through a gradient-based minimizer that iteratively updates the set of unknowns x_e driven by the current values of the objective function and its sensitivity [15]. Filtered sensitivities are provided to the minimizer in order to avoid numerical instabilities such as mesh dependence and the arising of checkerboard patterns.

Solving Eqn. (5), a black-and-white map is found that allow sketching the topology of a microstructure made of beam-like members that maximizes the ratio u_{out}/u_{in}. This preliminary layout is used to formulate a size optimization problem looking for the set of geometrical parameters that provides the expected ratio u_{out}/u_{in}.

In Figure 4 we show two black and white maps obtained from the optimization code: they differ from each other for the different boundary conditions we applied during the optimization process. Note that we are computing only a quarter of the structure (boundary conditions of symmetry are considered) and we are imposing some passive elements in the bottom and in the right side of the initial mesh: in that way we garantee the possibility of having a proof mass attached to that parts.

In Figure 4a the topology optimization starts with only one input spring sited in the middle of the passive elements area imposed in the bottom and with only one output spring sited in the middle of passive elements area imposed on the right. In Figure 4b, instead, we have three input springs in the passive elements area in the bottom and three output springs in the passive elements area on the right side.

3.1 Non-linear analysis of the optimized structure

Starting from the black and white map of Figure 4a, an ANSYS© model is done. As for the re-entrant honeycomb structure, we run a non-linear analysis to validate the results coming from the

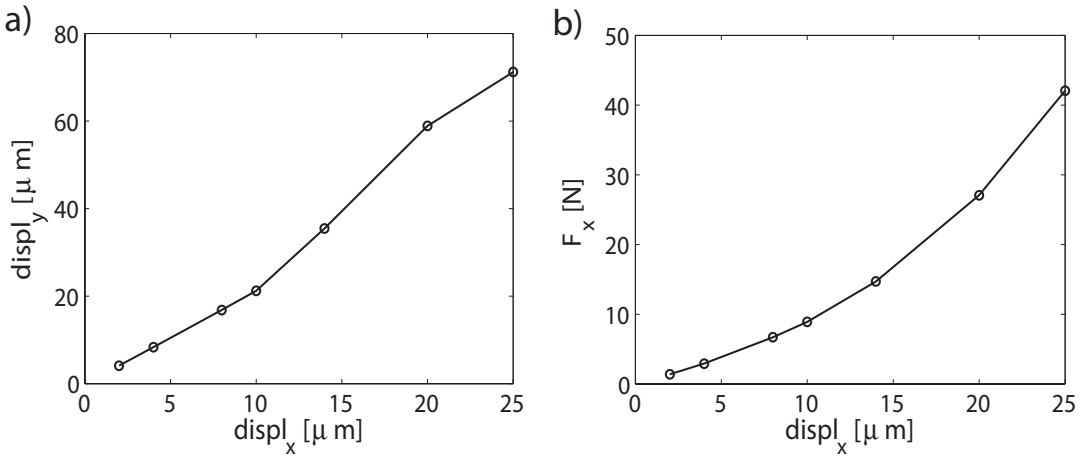

Figure 5: Numerical analysis of the auxetic structure optimized through topology optimization (numerical values are computed using the polysilicon as material). a) Imposed x-axis displacements versus obtained y-axis displacement: the relation is more than linear till an asymptotic behavior; b) imposed x-axis displacements versus computed x-axis reaction forces: for displacements of the order of some micrometers the relation is linear (fitting curve from 0 μm to 10 μm: $y = 9 \cdot 10^{-16}x^3 + 0.0275x^2 + 0.61x + 0.05$).

optimization procedure which use the small displacements hypothesis.

In Figure 5a we plot the relation between the applied x-axis displacements and the y-axis displacements obtained thanks to the auxetic behavior of the structure.

The relation is linear till x-axis imposed displacements are less than 10 μm and then become non-linear. For x-axis displacements higher than 25 μm a constant value of y-axis displacements is observed and this is due to the possibility of the structure itself to be deformed.

Note that the angular coefficient of the linear part of the relation is much higher than 1 and that means we are effectively amplifying the motion as whished.

In Figure 5b we plot the relation between the x-axis imposed displacements and the computed reaction forces. Since the applied displacements are smaller than 10 μm the relation is linear, when they become bigger some non-linearities arise.

Summarizing, starting from the geometry reported in Figure 4a, we can obtain a motion convertion and amplification. The linear range is garanteed for imposed displacements smaller than 10 μm for which we have an amplification factor of two (see Figure 5a).

4 Conclusions

In this work we investigate the behavior of auxetic structures through two different optimization procedures. The first optimization process starts from a re-entrant honeycomb structure and optimizes the geometry to reach a Poisson's ratio equal to -1 while the second one applies the topology optimization to minimize the value of the Poisson's ratio.

In both cases a numerical non-linear analysis is performed to validate the results coming from the optimization code which uses the small displacements hypothesis and in both cases a good linearity

is found for a displacements range of about ten micrometers which is, for example, the range actually used for the driven motion of gyroscopes.

The two structures can then be integrated into MEMS devices as motion conversion springs or motion conversion and amplification springs. The main problem of these structures is connected to the values of the reaction forces (see Figures 2b and 5b): they are too big for MEMS applications. Up to now we are working on different optimization models with the purpose to reduce the reaction forces exerted in the direction of the imposed displacements.

In this work we didn't care about the value of the reaction force because we were mostly interested in the linearity of the overall behavior.

Another open issue is connected to the possibility of going down with the dimension in the 3D printing technology, up to now we can only produce prototype at the mesoscale as shown in Figure 3, but we are working in this direction because the 3D-printing technology could release some constraints in the fabrication process of MEMS and allow a fast improvement of MEMS performances.

References

[1] Yang, W., Li, Z.-M., Shi, W., Xie B.-H. and Yang M.-B., "Review On auxetic materials", *J. of Mater. Science*, **Vol 39**, page 3269-3279 (2004).

[2] Larsen, U. D., Sigmund O. and Bouwstra, S., "Design and Fabrication of Compliant Micromechanisms and Structures with Negative Poissons Ratio", *J. of Microelectromech. Systems*, **Vol 6**, page 99-105 (1997).

[3] Elipe, J. C. A. and Lantada, A. D., "Comparative study of auxetic geometries by means of computer-aided design and engineering", *Smart Mater. Struct*, **Vol 21**, page 1-12 (2012).

[4] Levy, O., Krylov, S. and Goldfarb I., "Design considerations for negative Poisson ratio structures under large deflection for MEMS applications", *Smart Mater. Struct*, **Vol 15**, page 1459-1466 (2006).

[5] Yang, D. U., Lee, S. and Huang, F. Y., "Geometric effects on micropolar elastic honeycomb structure with negative Poissons ratio using the finite element method", *Finite Elements in Analysis and Design*, **Vol 39**, page 187-205 (2003).

[6] Critchley, R., Corni, I., Wharton, J. A., Walsh, F. C., Wood, R. J. K. and Stokes, K. R., "The Preparation of Auxetic Foams by Three-Dimensional Printing and Their Characteristics", *Advanced Eng. Mater*, **Vol 15**, page 980-985 (2013).

[7] Wang, M., C., Jiao, J., W., Yan, P., L., Mi, B., W. and Qin S., "A novel tri-axis MEMS gyroscope with in-plane tetra-pendulum proof masses and enhanced sensitive springs", *J. Micromech. Microeng.*, **Vol 24**, 045002 (10pp) (2014).

[8] Vigna, B., "Tri-axial MEMS Gyroscopes and Six Degree-Of-Freedom Motion Sensors", *IEEE International Electron Devices Meeting*, 5-7 December, 2011, Washington DC, United States.

[9] Hotzen, I., Ternyak, O., Shai, S. and Elata D., "Mass-fabrication compatible mechanism for converting in-plane to out of plane motion", *MEMS 2015*, 18-22 January,2015, Estoril, Portugal.

[10] Corigliano, A., De Masi, B., Frangi, A., Comi, C., Villa, A. and Marchi, M., "Mechanical characterization of epitaxial silicon through on chip tensile tests", *Journal of Microelectromechanical Systems*, **Vol 13**, page 200-219 (2004).

[11] Janus-Michalska, M., "Micromechanical model of auxetic cellular materials", *J. of Theoretical and Applied Mechanics* **Vol 47**, Warsaw (2009).

[12] Bendsøe, M.P. and Sigmund, O., "Topology optimization theory, methods and applications", New York, Springer (2003).

[13] Sigmund, O., "On the Design of Compliant Mechanisms Using Topology Optimization", *Mechanics of Structures and Machines* **Vol 25** , page 493-524 (1997).

[14] Bendsøe, M.P., "Optimal shape design as a material distribution problem", *Structural Optimization*, **Vol 1**, page 193-202 (1989).

[15] Svanberg, K., "Method of moving asymptotes-a new method for structural optimization", *International Journal for Numerical Methods in Engineering*, **Vol 24**, page 359-373 (1987).